J|A|C|S ARTICLES

Published on Web 12/05/2008

Photoswitchable Catalysts: Correlating Structure and Conformational Dynamics with Reactivity by a Combined Experimental and Computational Approach

Ragnar S. Stoll,[†] Maike V. Peters,[†] Andreas Kuhn,[†] Sven Heiles,[‡] Richard Goddard,[§] Michael Bühl,*[,⊥] Christina M. Thiele,*[,‡] and Stefan Hecht*[,†]

Department of Chemistry, Humboldt-Universität zu Berlin, Brook-Taylor-Strasse 2, 12489 Berlin, Germany, Max-Planck-Institut für Kohlenforschung, Kaiser-Wilhelm-Platz 1, 45470 Mülheim an der Ruhr, Germany, School of Chemistry, North Haugh, University of St. Andrews, St. Andrews, Fife KY16 9ST, U.K., and Clemens Schöpf Institut für Organische Chemie and Biochemie, Technische Universität Darmstadt, Petersenstrasse 22, 64287 Darmstadt, Germany

Received September 29, 2008; E-mail: buehl@st-andrews.ac.uk; cmt@punk.oc.chemie.tu-darmstadt.de; sh@chemie.hu-berlin.de

Abstract: Photocontrol of a piperidine's Brønsted basicity was achieved by incorporation of a bulky azobenzene group and could be translated into pronounced reactivity differences between ON- and OFF-states in general base catalysis. This enabled successful photomodulation of the catalyst's activity in the nitroaldol reaction (Henry reaction). A modular synthetic route to the photoswitchable catalysts was developed and allowed for preparation and characterization of three azobenzene-derived bases as well as one stilbene-derived base. Solid-state structures obtained by X-ray crystal structure analysis confirmed efficient blocking of the active site in the *E* isomer representing the OFF-states, whereas a freely accessible active site was revealed for a representative *Z* isomer in the crystal. To correlate structure with reactivity of the catalysts, conformational dynamics were thoroughly studied in solution by NMR spectroscopy, taking advantage of residual dipolar couplings (RDCs), in combination with comprehensive DFT computational investigations of conformations and proton affinities.

Introduction

Photocontrol over reactivity is an attractive task since a number of possible applications can be envisioned.[1] Catalysis is of particular interest due to the potential of amplifying the light stimulus by exploiting the catalytic cycle to enhance the efficiency of the overall chemical process. Reversible control can only be achieved by incorporating suitable photochromic gates, to allow driving the photoswitchable catalyst between (at least) two states of different ground-state reactivity. It is important to note that this approach is conceptually different to irreversibly photoactivated, i.e. caged, catalysts as well as photocatalysts.[2] The noninvasive character of light, in combination with the exceptional temporal and spatial control attainable, distinguishes it as an ideal external stimulus.

Almost all examples describing the photocontrol of catalytic processes rely on geometrical changes of the catalyst's backbone that alter its interaction with the substrate.[3,4] Although some photoswitchable catalyst systems have been described, no general and broadly applicable systems have yet been reported. We therefore decided to develop a conceptually new approach toward photoswitchable catalysts (Figure 1a).[5] Our concept is based on the reversible steric shielding of the catalyst's active site by a suitable blocking group, which can be moved away from the reactive center using a photochromic linker. A two-

[†] Humboldt-Universität zu Berlin.
[‡] Technische Universität Darmstadt.
[§] Max-Planck-Institut für Kohlenforschung.
[⊥] University of St. Andrews.

(1) (a) *Molecular Switches*; Feringa, B. L., Ed.; Wiley-VCH: Weinheim, 2001. (b) Balzani, V.; Venturi, M.; Credi, A. *Molecular Devices and Machines*; Wiley-VCH: Weinheim, 2008. (c) Kay, E. R.; Leigh, D. A.; Zerbetto, F. *Angew. Chem., Int. Ed.* **2007**, *46*, 72–191. (d) *Photochromism: Molecules and Systems*; Dürr, H., Bouas-Laurent, H., Eds.; Elsevier: Amsterdam, 2003. (e) Special Issue: Photochromism: Memories and Switches. Irie, M. *Chem. Rev.* **2000**, *100*, 1683–1890. (f) *Organic Photochromic and Thermochromic Compounds*; Crano, J. C., Guglielmetti, R. J., Eds.; Plenum Press: New York, 1999. (g) *Organic Photochromes*; El'tsov, A. V., Ed.; Consultants Bureau: New York, 1990. (h) Mayer, G.; Heckel, A. *Angew. Chem., Int. Ed.* **2006**, *45*, 4900–4921. (i) *Dynamic Studies in Biology*; Goeldner, M., Givens, R., Eds.; Wiley-VCH: Weinheim, 2005. (j) Willner, I. *Acc. Chem. Res.* **1997**, *30*, 347–356. (k) Willner, I.; Rubin, S. *Angew. Chem., Int. Ed. Engl.* **1996**, *35*, 367–385. (l) Hecht, S. *Small* **2005**, *1*, 26–28.

(2) (a) Parmon, V. N. *Catal. Today* **1997**, *39*, 137–144. (b) Esswein, A. J.; Nocera, D. G. *Chem. Rev.* **2007**, *107*, 4022–4047. (c) Palmisano, G.; Augugliaro, V.; Pagliaro, M.; Palmisano, L. *Chem. Commun.* **2007**, 3425–3437. (d) Hoffmann, M. R.; Martin, S. T.; Choi, W.; Bahnemannt, D. W. *Chem. Rev.* **1995**, *95*, 69–96. (e) Linsebigler, A. L.; Lu, G.; Yates, J. T., Jr. *Chem. Rev.* **1995**, *95*, 735–758.

(3) (a) Ueno, A.; Takahashi, K.; Osa, T. *Chem. Commun.* **1980**, 837–838. (b) Ueno, A.; Takahashi, K.; Osa, T. *Chem. Commun.* **1981**, 94–95. (c) Würthner, F.; Rebek, J., Jr. *Angew. Chem., Int. Ed. Engl.* **1995**, *34*, 446–448. (d) Würthner, F.; Rebek, J., Jr. *J. Chem. Soc., Perkin Trans. 2* **1995**, *172*, 7–1734. (e) Sugimoto, H.; Kimura, T.; Inoue, S. *J. Am. Chem. Soc.* **1999**, *121*, 2325–2326. (f) Cacciapaglia, R.; Di Stefano, S.; Mandolini, L. *J. Am. Chem. Soc.* **2003**, *125*, 2224–2227. (g) Sud, D.; Norsten, T. B.; Branda, N. R. *Angew. Chem., Int. Ed.* **2005**, *44*, 2019–2021.

(4) The only exception relates to a photoswitchable Lewis acid; however, no catalysis was reported. Lemieux, V.; Spantulescu, M. D.; Baldridge, K. K.; Branda, N. R. *Angew. Chem., Int. Ed.* **2008**, *47*, 5034–5037.

(5) Peters, M. V.; Stoll, R. S.; Kühn, A.; Hecht, S. *Angew. Chem., Int. Ed.* **2008**, *47*, 5968–5972.

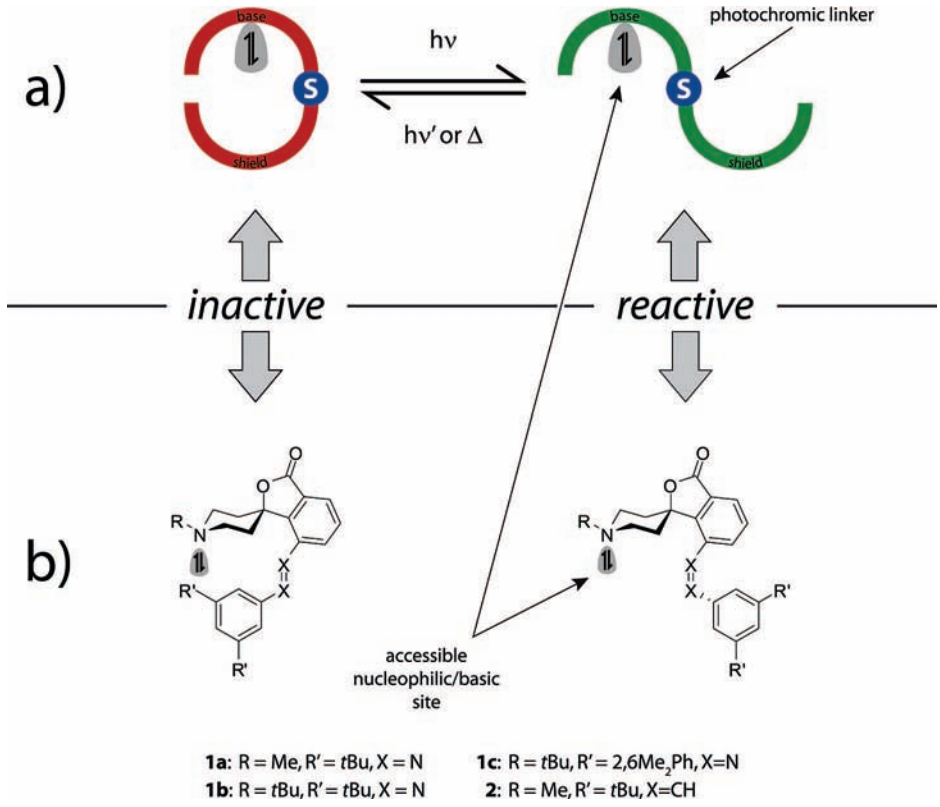

Figure 1. (a) Concept of reversible steric shielding of a catalyst's active site; (b) schematic representation of a photoswitchable piperidine base.

state catalyst system is obtained that can be driven between the ON-state, having an active site freely accessible for substrate molecules, and the OFF-state, which is sterically blocked and therefore inactive. To maintain the desired photochromic reactivity, other chromophores, potentially leading to detrimental energy transfer processes, should be excluded.[6]

As a first step toward this ambitious goal, we recently described the first prototype of a photoswitchable base (Figure 1b),[5] potentially enabling photocontrol over a large variety of general base-catalyzed reactions. Significant changes of Brønsted basicity upon isomerization of an azobenzene blocking group fused to a rigidified piperidine framework were demonstrated and exploited to control the activity as a general base catalyst. The accessibility to the basic site was conformationally restricted using a locked piperidine chair in combination with a spiroannulated azobenzene photochrome carrying a bulky shield. Herein, we give a detailed experimental and theoretical analysis of the conformational behavior of various generations of our catalyst system, enabling a comprehensive discussion of their photochromic behavior, structural dynamics, and resulting structure−reactivity relationships.

Results and Discussion

Synthesis. A modular synthesis of photoswitchable bases **1a**−**c** and **2** was developed to facilitate variation of key substituents at both the piperidine's N-atom and the terminal phenyl moiety of the azobenzene in order to tune the properties of the catalyst (Scheme 1). Azobenzene-based piperidine catalysts **1a**−**c** were readily assembled by a two-step procedure involving Pd-catalyzed *N*-arylation of spiroannulated piperidines **3a**,**b** with BOC-protected hydrazines **4a**,**b** followed by oxidative deprotection, while stilbene-based catalyst **2** was prepared via Suzuki cross-coupling of spiroannulated piperidine **3a** with styryl boronic ester **5**.[7]

Structure and Conformational Dynamics. If the concept of reversible steric shielding is to be applicable to the photocontrol of the activity of a catalyst, then a large structural change between ON- and OFF-states is required. Single crystals suitable for X-ray structural analysis of *E*-**1**, representing the OFF-states, and crystals of *Z*-**1b**, representing the ON-state were obtained, and their structures were determined. Figure 2 shows a superposition of the benzofuranone moieties of *E*-**1a**−**c** as well as *Z*-**1b**. Remarkable is the similarity of the structures *E*-**1a**−**c**, despite completely different crystal environments (root-mean-square deviation of the diazo-piperidyl-phthalide units: 0.1 Å). In the case of the crystal structure of *E*-**1b** there are three independent molecules in the asymmetric unit which differ only in the conformation of the methyl groups (root-mean-square deviation of non-methyl atoms: 0.2 Å). The common structural features of all structures *E*-**1** are (1) the placement of the blocking group directly in front of the lone pair of the nitrogen atom, with shortest intramolecular N−C distances 4.1−4.5 Å in the three structures; (2) the chair conformation of the piperidine ring, to within 0.02 Å; and (3) the perpendicular relationship between the benzofuranone unit and the piperidine mean ring plane (mean angle: 89°). Clearly, the blocking group takes up a position, which efficiently shields the lone pair of the piperidine N-atom.

In the case of the *Z* isomer (green in Figure 2), the azobenzene moiety has a torsion angle 7.1°, and the blocking group is moved away from the active site of the catalyst, leaving the active site

(6) (a) Peters, M. V.; Goddard, R.; Hecht, S. *J. Org. Chem.* **2006**, *71*, 7846–7849. (b) Peters, M. V.; Stoll, R. S.; Goddard, R.; Buth, G.; Hecht, S. *J. Org. Chem.* **2006**, *71*, 7840–7845.

(7) See Supporting Information.

Scheme 1. Synthesis of Azobenzene-Derived Catalysts **1a**−**c** and Stilbene-Derived Catalyst **2**

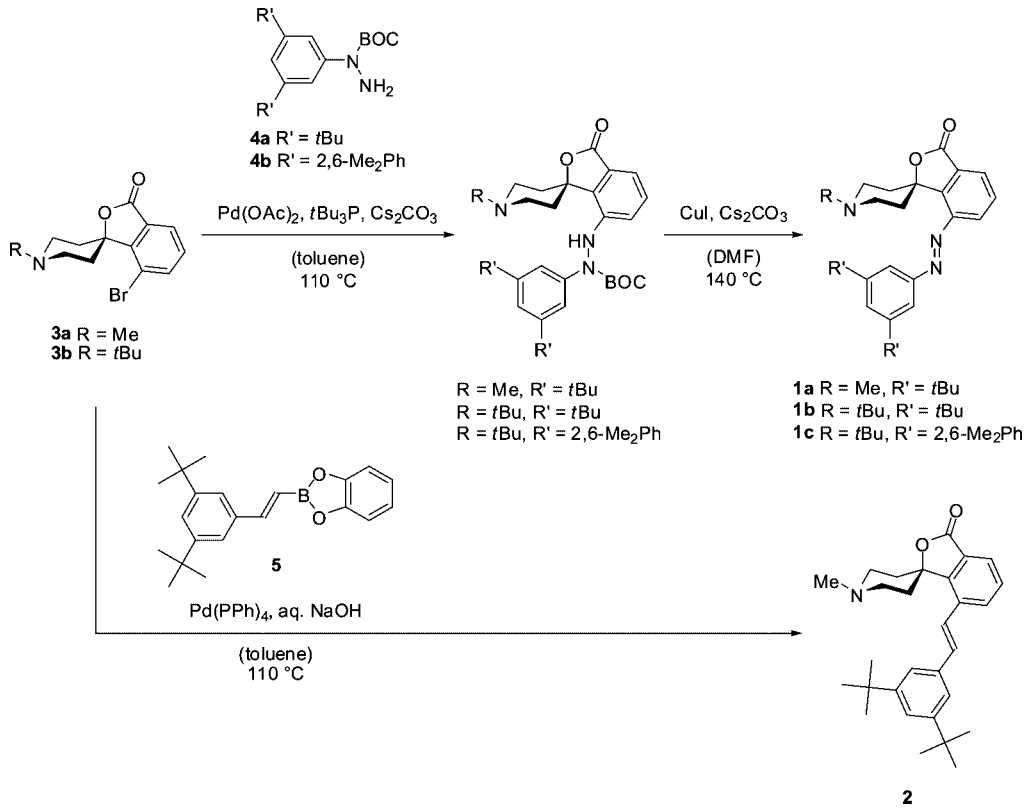

freely accessible for reaction as intended in our design. The intramolecular N−C distance of the lone pair of the piperidine to the nearest *tert*-butyl group of the phenyl moiety is 7.1 Å, and therefore the substituents on the phenyl ring no longer provide a barrier. Otherwise, the conformation of the piperidine-benzofuranone moiety is essentially similar to those seen in *E*-**1a**−**c**. The conformation of the piperidine in all four crystal structures is such that the N-lone pair points away from the lone pairs on the furanone ring O-atom, in line with the less destabilizing 1,3-diaxial interactions of the two piperidine 2,6-H-atoms with the 4-carbonyloxy substituent of the lactone as compared to the alternative larger phenyl substituent of the benzofuranone. X-ray analysis, however, only provides a static picture of the structural situation in the solid state; thus, for a thorough understanding of the reactivity of catalysts *E*-**1a**−**c** and *Z*-**1** it is necessary to investigate their structure and conformational behavior in solution, hence gaining detailed insights into the dynamics of the systems.

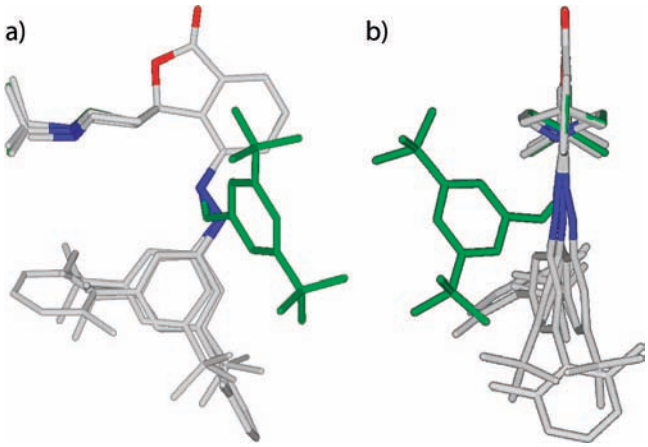

Figure 2. Overlay of X-ray crystal structures of catalysts *E*-**1a**−**c** and *Z*-**1b** (green): (a) side view (projection onto the plane of the benzofuranone moiety); (b) rear view.

To achieve the desired control over the accessibility of the basic/nucleophilic piperidine N-atom's lone pair, it is necessary to dictate both configuration (path a in Scheme 2) as well as conformation (paths b−d in Scheme 2) of the interconvertible *E* and *Z* isomers. Control of the latter one is a much more difficult task due to the complex dynamics under the reaction conditions. We therefore investigated **1** in solution by NMR spectroscopic methods, in particular, variable-temperature NMR,[8] EXSY,[9] and the recently introduced residual dipolar couplings (RDCs),[10] in combination with computational studies (Table 1).

Inversion at the piperidine's N-atom (blue path b in Scheme 2) is of particular interest, because the concomitant exchange of equatorial alkyl group and axial lone pair in *E*-**1** exposes the latter to the environment, potentially bestowing residual catalytic activity on the formal OFF-state. The computed *N*-inversion barrier via **1**-TSi is rather similar for all bases, amounting to approximately 7−8 kcal/mol (Table 1). As expected, the N-inverted isomers i-**1** carrying an axial substituent R are significantly higher in energy than the equatorial ground state. The species with the smallest R, i-**1a**, is least disfavored by ∼4 kcal/mol, according to DFT,[11] whereas the increased bulk of that group in i-**1b** and i-**1c** results in further destabilization by approximately 1−3 kcal/mol (Table 1).

(8) Kessler, H. *Angew. Chem., Int. Ed. Engl.* **1970**, *9*, 219–235.
(9) Perrin, L.; Dwyer, T. J. *Chem. Rev.* **1990**, *90*, 935–967.
(10) (a) Thiele, C. M.; Berger, S. *Org. Lett.* **2003**, *5*, 705–708. (b) Thiele, C. M. *Concepts Magn. Reson.* **2007**, *30A*, 65–80. (c) Thiele, C. M. *Eur. J. Org. Chem.* **2008**, *24*, 5673–5685.

Scheme 2. Schematic Representation of Selected Local Minima and Transition States Investigated by DFT Calculations

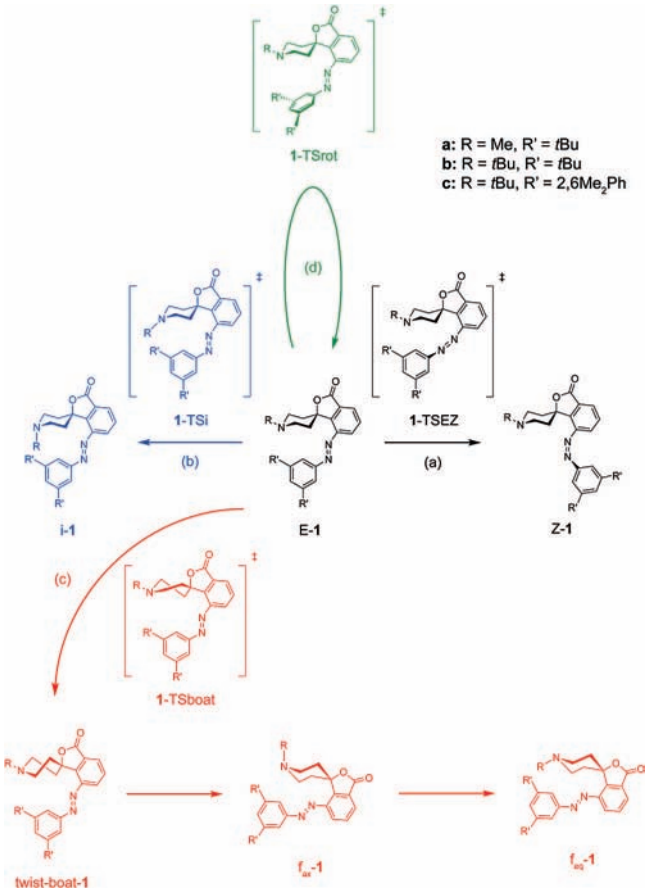

It is not straightforward to investigate N-inversion experimentally. For *N*-methyl-substituted piperidines, ^{13}C chemical shifts for the *N*-methyl carbon for axial and equatorial methyl groups have been reported.[12] However, the chemical shift of the only *N*-methyl signal observed for *E*-**1a**, δ (^{13}C) = 45.6 ppm, lies exactly in between those two values and does not change position or line shape even when lowering the temperature to 178 K. This observation can have two possible explanations: either only one conformer is mainly populated (no change in signal position and line shape) or N-inversion is fast on the NMR time scale even at low temperatures (chemical shift in between those reported for axial and equatorial *N*-methyl groups). As we did not obtain conclusive experimental results for **1a**, we decided to conduct a more detailed structural and dynamical NMR investigation on the *E* isomer of the catalytically more active system **1b**.

We used residual dipolar couplings (RDCs) for this purpose, as the other conformationally relevant NMR-parameters (NOE, *J* couplings) are not expected to lead to unequivocal results. If only dipolar couplings of directly bonded nuclei (^1D) are used for the determination of the spatial structure of rigid compounds, RDCs can be used as angular restraints.[10] In this case we use $^1D_{C-N}$ (coupling between the quaternary carbon of the *N*-*tert*-butyl group and the piperidine N-atom) to determine the orientation of the *N*-*tert*-butyl group with respect to the piperidine ring, thus yielding information on N-inversion. Usually $^1D_{C-N}$ cannot be measured easily, yet in the case of **1b**, it can be determined indirectly from the $^1D_{C-H}$ coupling of the rotatable *tert*-butyl groups (attached to the piperidine N-atom and the steric blocker).[7] The structural proposal, fitting the experimentally derived RDCs best, can be considered as accurate representation of the spatial structure in solution.[10b,c]

Table 1. Potential Energies ΔE (in parentheses: Free Energies ΔG)[a] of Selected Isomers and Transition States of **1a**−**c**

	a	b	c
E-**1**	0.0 (0.0)	0.0 (0.0)	0.0 (0.0)
1-TSEZ	39.8 (37.6)	39.6 (37.6)	40.1 (38.0)
Z-**1**	15.8 (14.8)	15.4 (15.8)	15.3 (15.0)
1-TSi	8.5 (7.4)	7.0 (8.2)	5.8 (7.2)
i-**1**	3.8 (4.0)	6.0 (7.1)	5.5 (5.4)
1-TSboat	11.6 (12.0)	11.5 (12.7)	n.a.
f_{ax}-**1**	7.2 (7.8)	9.0 (10.9)	n.a.
f_{eq}-**1**	7.0 (7.6)	7.4 (8.7)	n.a.
1-TSrot	7.7 (7.0)	7.5 (6.9)	6.9 (5.6)

[a] In kcal/mol relative to *E*-**1** isomer, B3LYP/6-31G* level.

Compound *E*-**1b** was oriented in a lyotropic liquid crystalline matrix of high-molecular weight PBLG[13] with $CDCl_3$ as organic cosolvent, and variable angle sample spinning (VASS)[14] was used to reduce RDCs to a suitable range, as strong coupling was observed between the diastereotopic protons of the piperidine methylene groups. This enabled us to measure all $^1D_{C-H}$ and even some long-range D_{H-H}. The geometry-optimized DFT structures of *E*-**1b** and i-**1b** were subsequently used to probe N-inversion. In order to distinguish between the two conformers, a scaling procedure had to be used such that $^1D_{C-N}$ gets approximately the same weight as $^1D_{C-H}$.[15] Two approaches of RDC data analysis were applied. First the respective coupling $^1D_{C-N}$, describing the orientation of the *tert*-butyl group with respect to the piperidine ring, was included in the fitting step using the DFT geometries of *E*-**1b** and i-**1b** and all RDCs except those of the steric blocker (*vide infra*).[7] Using this procedure, a significantly better fit was obtained for *E*-**1b** (quality factor $q = 0.131$) than for i-**1b** ($q = 2.046$). This already suggests that the N-inverted isomer i-**1b** is not significantly populated, whereas the proposed structure *E*-**1b** is matched extremely well by the experimental RDCs (Figure 3b). To independently confirm our findings, a second kind of analysis was performed by excluding $^1D_{C-N}$ from the fitting procedure and predicting its value from the orienting tensor of the rest of the compound[16] (again without using the data of the steric blocker). The predicted $^1D_{C-N}$ value of −24.1 Hz for *E*-**1b** is in good agreement with the measured coupling of -36 ± 18 Hz as compared to the

(11) A similar energy difference has been obtained between equatorial and axial *N*-methyl piperidine, 3.9 kcal/mol at the MP2/cc-pVTZ level: Dos Santos, F. P.; Tormena, C. F *J. Mol. Struct. (THEOCHEM)* **2006**, *763*, 145–148.

(12) Crowley, P. J.; Robinson, M. J. T.; Ward, M. G. *Tetrahedron* **1977**, *33*, 915–925.

(13) Marx, A.; Thiele, C. M. *Chem. Eur. J.* **2008**, http://dx.doi.org/10.1002/chem.200801147.

(14) Thiele, C. M. *Angew. Chem., Int. Ed.* **2005**, *44*, 2787–2790.

(15) The two conformers could initially not be distinguished because of a fitting problem as $^1D_{C-N}$ becomes very small (because of the small gyromagnetic ratios) and the PALES program (Zweckstetter, M.; Bax, A. *J. Am. Chem. Soc.* **2000**, *122*, 3791−3792) used for fitting the data does not allow for weighing of couplings within the fitting procedure, resulting in equally good fits for *E*-**1b** and i-**1b**. To obtain conclusive results, the corresponding coupling was scaled by a factor of 1000, while the bond length was reduced in the coordinate file to 10% of its original value using the program MolArch+. (Immel, S. *MolArch+*, Molecular architecture modelling program; Universität Leipzig: Leipzig, 2008.) As ^1D is proportional to $1/r^3$ the physical information of $^1D_{C-N}$ is unchanged by this procedure.

(16) This method is described in: Thiele, C. M. *J. Org. Chem.* **2004**, *69*, 7403−7413.

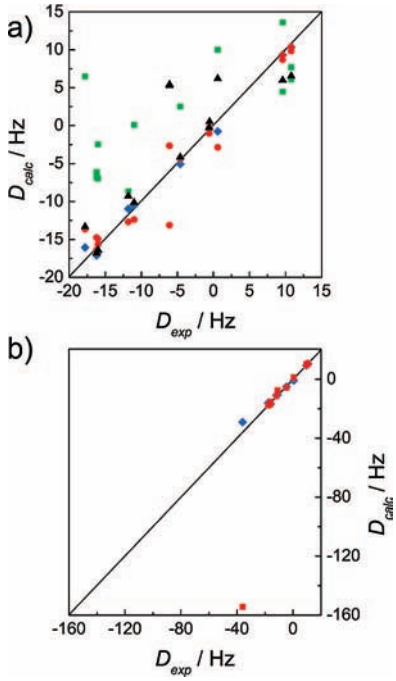

Figure 3. Comparison of RDCs calculated (D_{calc}) for the different possible conformational states of *E*-**1b** with the ones observed experimentally (D_{exp}). In (a) the fit for the equilibrium structure *E*-**1b** (blue diamonds, without using the data from the steric blocker) is depicted together with the ring-flipped f_{eq}-**1b** (green squares). The red dots show the fit for all data (including the RDCs of the steric blocker) to *E*-**1b**, the black triangles to the transition structure for the rotation of the steric blocker **1b**-TSrot. In (b) the fit for the equilibrium structure *E*-**1b** (blue diamonds, without using the data from the steric blocker, the C−N bond length reduced to 10% of its original length, see text) is compared to the N-inverted i-**1b** (red squares).

value of −248.8 Hz predicted for i-**1b**.[15] Therefore, from analysis of our RDC data we can unequivocally conclude that no significant population of the N-inverted conformer i-**1b** could be detected by NMR spectroscopy.

Inversion of the six-membered piperidine chair, i.e. ring "flip" (red path c in Scheme 2), represents another possible mechanism to render the axial lone pair in *E*-**1** accessible to the environment, thereby constituting a potential source of residual catalytic activity of the formal OFF-state. This ring flip is expected to proceed via one or more twist-boat intermediates to the ring-inverted form f_{ax}-**1**, which via N-inversion can subsequently rearrange to isomer f_{eq}-**1** with equatorial R and an exposed N-lone pair. After conformational analysis of the parent *N*-methyl piperidine at the B3LYP/6-31G* level,[7] selected stationary points along this path were located for **1a** and **1b**, focusing on the final product and a representative transition state leading to a twist-boat (or twist) isomer. As expected, the ring-flipped isomers f_{eq}-**1a**,**b** are strongly disfavored, by ∼7−9 kcal/mol, and are accessible only via significant barriers, up to ∼12−13 kcal/mol (Table 1).[17] Incidentally, these numbers are close to the corresponding barrier for cyclohexane.[18] Overall, there is no indication from the computations that ring-flipped isomers could be populated to any significant extent. Very similar results are to be expected for the bulky derivative **1c**, which was not further studied computationally.

Compounds *E*-**1a** and *E*-**1b** were investigated experimentally, and inspection of their ^{1}H NMR spectra shows that both pairs of diastereotopic protons of the piperidine methylene groups are anisochronous, indicative for locked chair conformations. These observations were further supported by EXSY experiments, revealing no exchange between these diastereotopic protons and thus excluding any significant population of ring-flipped isomers f_{eq}-**1a**,**b**. Final confirmation of the absence of chair inversion was obtained by fitting the RDC data for *E*-**1b** to the DFT geometries of *E*-**1b** and its corresponding ring-flipped conformer f_{eq}-**1b**. As expected, the computed structure *E*-**1b** is in excellent agreement with the RDC data ($q = 0.067$, see Figure 3a, blue diamonds), whereas alternative structure f_{eq}-**1b** results in a poor fit ($q = 0.823$, see Figure 3a, green squares).

Finally, rotation of the aromatic blocking group $C_6H_3R'_2$, about the N−C axis (green path d in Scheme 2) represents a fluxional process that could potentially affect the accessibility of the piperidine lone pair in *E*-**1**. The fact that this process is rapid at ambient temperature, at least on the NMR time scale, is already suggested by the equivalence of the two R′ moieties in the NMR spectra. As the signals could be isochronous[19] by coincidence, detailed analysis of our collected RDC data for *E*-**1b** was carried out, and conformational flexibility became apparent. Observed RDC values are usually smaller for flexible parts of the compound (due to averaging), and RDCs do not fit any of the structural proposals,[20] as observed when fitting the complete set of RDCs to the DFT-structure of *E*-**1b** ($q = 0.215$, see Figure 3a, red dots). Furthermore, the calculated $^1D_{C-H}$'s for the two ortho protons of the steric blocker in the case of a rigid structure (−13.1 and −2.6 Hz) deviate largely from the measured averaged $^1D_{C-H}$ value (−6.1 Hz), confirming fast rotation on the NMR time scale.[7,21]

In accordance with these observations, only modest barriers ranging between 6−8 kcal/mol (Table 1) were computed for this rotation involving **1**-TSrot (green path d in Scheme 2). Interestingly, the lowest barrier was computed for the largest substituent. Indeed, visual inspection of the *E*-**1c** ground state shows that no serious clash between the R and R′ groups is to be expected upon rigid rotation of the blocking group. Despite the comparably low hindrance toward blocking-group rotation in *E*-**1a**, *E*-**1b**, and *E*-**1c**, the bulky R′ groups in the latter appear to be more effective in shielding the lone pair than those in the former (see discussion of reactivities below).

Photochromism. The photochromic behavior of photoswitchable piperidine bases **1a**−**c** and **2** was investigated in detail (Table 2). Azobenzene-based catalysts **1a**−**c** showed the expected isomerization behavior upon irradiation of the thermally stable *E* isomers. As evident from UV/vis spectra, irradiation with light of 365 nm wavelength leads to a decrease in intensity of the absorption band at about 330 nm, which is

(17) There are many more possible twist or twist-boat intermediates and transition states, depending on which C−C or C−N bond in the ring is rotated relative to its opposite counterpart and in what direction. We have refrained from locating all of them, but from the present results it is already clear that the overall barrier must be in the interval between ∼7−13 kcal/mol, implying notable activation for this process.

(18) For example: ΔE = 11.4 kcal/mol at B3LYP/6-31G* for the C_2-symmetric twist-chair transition state (or half-chair), cf. structure **10** in the following reference, where a value of 11.9 kcal/mol has been obtained at MP2/6-31G* Leong, M. K.; Mastrryukov, V. S.; Boggs, J. E. *J. Phys. Chem.* **1994**, *98*, 6961–6966.

(19) Leuthäusser, S.; Schmidts, V.; Thiele, C. M.; Plenio, H. *Chem. Eur. J.* **2008**, *14*, 5465–5481.

(20) Another indication is given by the fact that we did not observe differentiation of enantiotopic faces, which is to be expected in a chiral orienting medium if no rotation of the steric blocker (converting one enantiotopic face into the other) is occurring.

(21) If the transition-state structure of this rotation, **1**-TSrot, is used, the quality of the fit is further reduced (q = 0.426, Figure 3a, black triangles).

Table 2. Photochromic Properties and Activation Parameters for Thermal $Z \rightarrow E$ isomerization of **1a**−**c** and **2**

	absorption		PSS composition		thermal Z → E isomerization			
	$\lambda_{max}(E)^a$ [nm]	$\lambda_{max}(Z)^b$ [nm]	$E \rightarrow Z$ (Z/E)	$Z \rightarrow E$ (Z/E)	$\tau_{1/2}{}^c$ [h]	$\Delta G^{\ddagger}{}_{298\ K}{}^d$ [kcal mol^{-1}]	$\Delta H^{\ddagger d}$ [kcal mol^{-1}]	$\Delta S^{\ddagger d}$ [cal mol^{-1} K^{-1}]
1a	335	444	90:10	15:85	268	26	23	−9
1b	335	444	90:10	15:85	286	25	22	−11
1c	333	440	95:5[e]	10:90	466	25	23	−8
2	298	279	93:7	78:22	−	−	−	−

[a] π,π^*-Absorption. [b] n,π^*-Absorption. [c] At 20 °C (293.15 K). [d] Obtained from kinetic data of the thermal $Z \rightarrow E$ isomerization at various temperatures and Eyring analysis of the data. [e] No E isomer was detected by UPLC analysis.[7]

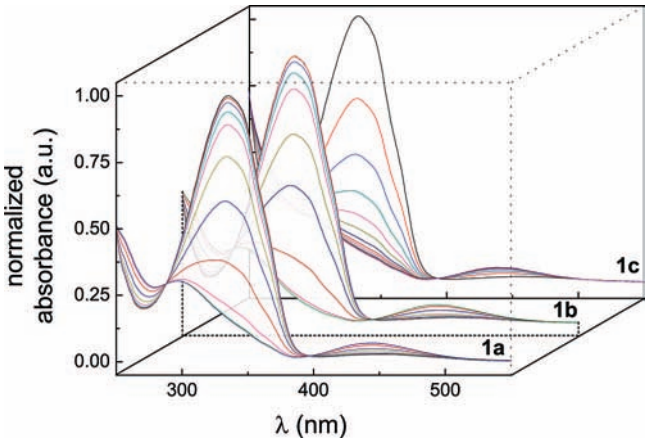

Figure 4. Absorbance spectra of **1a**−**c** in acetonitrile taken at varying intervals during irradiation with light of 365 nm wavelength (**1a**: 2.8×10^{-5} M, 12:48 min irradiation time; **1b**: 3.1×10^{-5} M, 12:46 min irradiation time; **1c**: 3.0×10^{-5} M, 14:00 min irradiation time). Spectra are normalized to the maximum n,π-absorption around 335 nm.

attributed to the π,π^*-transition of the azobenzene chromophor, along with an increase of the band around 450 nm, which is attributed to the n,π^*-absorption (Figure 4).[1d,g] Irradiation of larger quantities of catalysts **1a**−**c** in acetonitrile solution allowed for isolation of samples containing mainly the Z isomers. X-ray crystal structure analysis of Z-**1b** shows a pronounced deviation from planarity of the azobenzene core, leading to significant electronic decoupling of both phenyl rings in the Z isomer (Figure 2) and the resulting hypsochromic shift of the π,π^*-absorption constitutes the basis of photochromism in azobenzenes. Photostationary states obtained by irradiation of analytical samples of **1a**−**c** show a remarkably high content of Z isomer, amounting to at least 90% according to UPLC analysis. The Z isomer can be converted to the E isomer photochemically by irradiation with visible light ($\lambda \geq 400$ nm). However, the extent of switching is smaller due to the non-negligible absorption of the E isomer above 400 nm and yields photostationary-state mixtures containing up to 90% E isomer in the case of **1c** and around 85% for **1a** and **1b**.

As expected for azobenzenes, catalysts **1a**−**c** thermally revert from the Z to the E isomer. Thermal half-lives $\tau_{1/2}$ observed for Z-**1a**−**c** were found to be extraordinarily extended as compared to the parent azobenzene ($\tau_{1/2} = 16$ h in benzene).[22] Thermal isomerization of Z-**1a** and Z-**1b** was observed to occur with half-lives of 268 and 286 h at 20 °C, respectively. Change of the steric demand of the blocking group by replacing the 3,5-di-*tert*-butylphenyl fragment with the 3,5-bis(2,6-dimethylphenyl)phenyl fragment further prolonged half-life to 466 h at 20 °C for Z-**1c**. Activation parameters for the thermal isomerization of Z-**1a**−**c** were determined by measuring the rate constants at different temperatures using UV/vis spectroscopy (Table 2).[23] All activation parameters obtained are in reasonable agreement with parameters determined for other azobenzene derivatives.[24]

Thermal isomerization was also investigated computationally. For **1a**, the only E/Z-transition state that could be located is one that is associated with inversion at the diazo-N-atom bound to the spiro-annulated core (**1a**-TSEZ, see black path a in Scheme 2).[25] That transition state was obtained even when the search started from a structure that would correspond to a rotation about the N═N axis. This finding is in line with earlier DFT results for azobenzene, according to which inversion has a lower barrier than rotation.[26] For the other derivatives, similar inversion transition states **1b**,**c**-TSEZ were found. In all of these, the 3,5-disubsituted benzene ring is oriented almost perpendicular to the plane of the spiro-annulated benzene ring having a C−N═N−C torsional angle around 100° and N═N−C−C torsional angles close to 0° and 180°, respectively. Activation parameters for $Z \rightarrow E$ isomerization in the gas phase, calculated as the free energy of **1**-TSEZ relative to that of Z-**1** (Table 1), are 22.8, 21.8, and 23.0 kcal/mol for **1a**, **1b**, and **1c**, respectively. These numbers are slightly lower than the experimental estimates for $\Delta G^{\ddagger}$ in Table 2 and show no particular trend. Enthalpies of activations $\Delta H^{\ddagger}$ are fairly equal when comparing theoretical[27] and experimental values, indicating a comparable enthalpic loss when going from the strained Z isomer to the twisted transition state. Activation entropies $\Delta S^{\ddagger}$ for the gas-phase reactions are small in all cases, suggesting that contributions to $\Delta S^{\ddagger}$ in the condensed phase are mostly associated with solvation effects. From the negative values found experimentally for $\Delta S^{\ddagger}$, it can be deduced that the degree of order of solvated Z-**1a**−**c** increases by going to its respective transition state.

With regard to the prolonged half-life of Z-**1c**, it is reasonable to assume a larger entropic contribution resulting in a decrease of $\Delta G^{\ddagger}$ ($\Delta G^{\ddagger} = \Delta H^{\ddagger} - T\Delta S^{\ddagger}$) compared to **1a**,**b**, because the larger, more hydrophobic blocking group is more weakly solvated therefore requiring a smaller amount of reorganization in the solvation sphere. The small increase in half-life observed experimentally for **1a** and **1b** is most likely due to a similar

(22) Schulte-Fröhlinde, D. *Liebigs Ann. Chem.* **1958**, *612*, 131–138.

(23) Please note, half lives reported in Table 2 were directly determined from the rate constants at the given temperature. Estimated errors for activation parameters are in the range of ±1 kcal mol^{-1} for $\Delta H^{\ddagger}$ and ±1 cal mol^{-1} K^{-1} for $\Delta S^{\ddagger}$. Rate constants and half lives, which can be calculated from $\Delta H^{\ddagger}$ and $\Delta S^{\ddagger}$ by the thermodynamic formulation of the Eyring equation, are extremely sensitive to these quantities.

(24) (a) Gegiou, D.; Muszkat, K. A.; Fischer, E. *J. Am. Chem. Soc.* **1968**, *90*, 3907–3918. (b) Le Fèvre, R. J. W.; Northcott, J. *J. Chem. Soc.* **1953**, 867–870.

(25) That this transition state indeed connects Z-**1a** and E-**1a** was verified by reoptimization at B3LYP/3-21G and following the intrinsic reaction coordinate (see: (a) Gonzalez, C.; Schlegel, H. B. *J. Chem. Phys.* **1989**, *90*, 2154–2161. (b) Gonzalez, C.; Schlegel, H. B. *J. Phys. Chem.* **1990**, *94*, 55235527) at that level.

(26) Crecca, C. R.; Roitberg, A. E. *J. Phys. Chem. A* **2006**, *110*, 8188–8203.

(27) The corresponding DFT values for $\Delta H^{\ddagger}$ (not included in Table 1) are 23.0, 22.9, and 23.6 kcal/mol for **1a**, **1b**, and **1c**, respectively.

Table 3. Basicities and Rate Constants of the Henry Reaction Obtained for Catalysts **1a**−**c** and **2**.

	basicities			Henry reaction				
	pK_a(OFF)[a]	pK_a(ON)[b]	ΔpK_a[c]	PSS[d](*Z*/*E*)	k_{OFF}[e] [10^{-6} s^{-1}]	k_{obs}[f] [10^{-6} s^{-1}]	k_{ON}[g] [10^{-6} s^{-1}]	k_{rel} (k_{ON}/k_{OFF})
1a	−	−	−	80:20	4.96	15.0	21.5	4.3
1b	15.9	16.7	0.8	90:10	0.963	8.87	12.7	13.2
1c	16.0	16.7	0.7	90:10	0.391	10.6	13.9	35.5
2	−	−	−	93:7	12.9	−	25.4	2.0

[a] pK_a-value of the *E* isomer representing the OFF-state. [b] pK_a-value of the photostationary state mixture representing the ON-state. [c] Difference of pK_a-values, i.e. pK_a(PSS) − pK_a(*E*). [d] Photostationary state obtained by preparative irradiations at $\lambda = 365$ nm. [e] Rate constant of Henry reaction using pure *E* isomer. [f] Rate constant of Henry reaction using the photostationary state mixture obtained by preparative irradiations at $\lambda = 365$ nm. [g] Rate constant of Henry reaction extrapolated to 100% *Z* isomer.

effect associated with the increase in hydrophobicity when exchanging the methyl substituent for the *tert*-butyl group. The effect is smaller, because the site of substituent exchange is more remote from the azo fragment causing differences in solvation having a smaller influence on the transition state of $E \rightarrow Z$ isomerization. In fact, experimentally determined values for $\Delta S^{\ddagger}$ increase by about 3 cal mol^{-1} K^{-1} going from **1a** to **1c**. However, this can only be seen as a trend and experimental uncertainties preclude any accurate quantification.

To avoid potential problems originating from the thermal instability of the *Z* isomer of the azobenzene-based catalysts **1a**−**c**, stilbene-based catalyst **2** was investigated. In contrast to azobenzene and its derivatives, stilbenes exhibit a photochromic behavior with both switching states being thermally stable (photochromism of the P type).[28] As expected, irradiation of **2** led to conversion of the *E* isomer to the *Z* isomer accompanied by a decrease of the absorption band around 300 nm and a small increase of absorption around 250 nm.[7] Remarkably, the photostationary state mixture obtained by irradiation of analytical samples in acetonitrile with light of wavelength greater than 330 nm contained almost exclusively *Z* isomer, i.e. 97% as determined by HPLC. As expected, thermal reversion of *Z*-**2** to *E*-**2** was not observed. Irradiation of the photostationary state mixture with light of 250 nm wavelength induced $Z \rightarrow E$ isomerization, yet only 22% *E* isomer could be recovered due to the marked absorption of the *E* isomer at 250 nm. No spectral region can be identified that would allow for satisfactory $Z \rightarrow E$ photoisomerization, since the *E* isomer's absorption is more significant throughout the entire wavelength range as compared to the *Z* isomer, precluding the use of **2** as a practical photoswitch. Implications of the small extent of $Z \rightarrow E$ switching on the catalytic performance of the stilbene catalyst **2** are discussed in the next section.

Reactivity.

Basicity. The photochromic behavior of catalysts **1a**−**c** is associated with pronounced structural changes, which translate into differences in chemical reactivity of both isomers. In context with the desired general base catalysis, the basicity of the amines and the extent to which it can be altered between the ON- and OFF-states are of great interest. A change in basicity upon isomerization could be expected due to the different stabilities of the corresponding acid−base adducts involved. However, it is important to note that the realization of a photoswitchable Brønsted base constitutes a formidable task since the proton represents the smallest possible electrophile and precludes strong steric interactions.

To compare the basicities of different switching states of compounds **1b**,**c**, titration experiments with trifluoromethanesulfonic acid were carried out. Negligible changes in the absorption spectra of **1b** and **1c** upon protonation precluded a direct determination of the concentrations of the nonprotonated and protonated forms, necessary for a direct evaluation of the pK_a-values. However, indirect determination of these concentrations was possible by using Neutral Red[29] (3-amino-7-dimethylamino-2-methylphenazine) as the reference base, having a pK_a of 15.6 for the protonated form in acetonitrile.[7] The choice of the reference base is crucial, since a too large difference in basicity of catalyst and reference base precludes meaningful measurements.[30] Indeed, pK_a-values of both isomers of **1b** differ significantly (Table 3). The basicity of *Z*-**1b** (ON-state) increased by almost 1 order of magnitude amounting to $pK_a = 15.9$ as compared to $pK_a = 16.7$ for the corresponding *E*-**1b** (OFF-state). For *E*-**1c** and *Z*-**1c** pK_a-values of 16.0 and 16.7, respectively, were found and are essentially identical to those of the respective **1b** analogues, when considering the uncertainty of these measurements of approximately ±0.1 pK_a units.

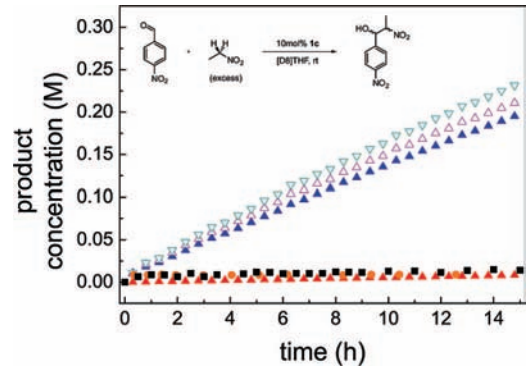

Figure 5. Catalytic performance of catalyst **1c** in the Henry reaction calculated from product concentrations determined from ^{1}H NMR spectroscopy (red ▲: *E*-**1c**, blue ▲: PSS:*Z*-**1c**:*E*-**1c** = 90:10, purple △: PSS with thermal correction for $Z \rightarrow E$ isomerization, green ▽: extrapolation to 100% *Z*-**1c**, black ■: no catalyst, orange ●: *E*-azobenzene).

General Base Catalysis. Reactivity differences associated with both switching states of compounds **1a**−**c** as well as **2** could be exploited to photocontrol the conversion in a general base-catalyzed reaction. For this purpose, the nitroaldol reaction, commonly referred to as Henry reaction,[31] of nitroethane with 4-nitrobenzaldehyde was investigated as a model reaction (Figure 5) due to its low background rate in the absence of base catalyst. Using an excess of the nitroethane substrate to ensure

(28) Bouas-Laurent, H.; Dürr, H. *Pure Appl. Chem.* **2001**, *73*, 639–665.
(29) (a) Leito, I.; Kaljurand, I.; Koppel, I. A.; Yagupolskii, L. M.; Vlasov, V. M. *J. Org. Chem.* **1998**, *63*, 7868–7874. (b) Kaljurand, I.; Rodima, T.; Leito, I.; Koppel, I. A.; Schwesinger, R. *J. Org. Chem.* **2000**, *65*, 6202–6208. (c) Biondic, M. C.; Erra-Balsells, R. *J. Chem. Soc. Perkin Trans.* **1997**, *7*, 1323–1327.
(30) For optimal results, the pK_a of the reference base should not differ more than 2 pK_a units from the pK_a of the base to be measured.
(31) (a) Henry, L. *C. R. Hebd. Seances Acad. Sci.* **1895**, *120*, 1265–1268. (b) For a recent review, consult: Luzzio, F. A *Tetrahedron* **2001**, *57*, 915–945.

pseudo-first-order kinetics, the buildup of *syn*- and *anti*-aldol products in the presence of 10 mol % of catalyst in [D_8]THF solution was monitored by ^{1}H NMR spectroscopy. Reactivity originating from the much less basic azochromophore could be ruled out by a control experiment using azobenzene itself as catalyst, leading to no acceleration of product formation (Figure 5). The catalysts employed in the kinetic experiments were used in their isolated form, i.e. the *E* isomer was used in its pure form, while the *Z* isomer was used as the photostationary-state mixture containing minor amounts of residual *E* isomer.[32] For comparison of the reactivity associated with the two switching states of a catalyst, k_{rel} was defined as the ratio of rate constants for use of either pure *Z* or pure *E* isomer, that is $k_{rel} = k_{ON}/k_{OFF}$. The rate constant for use of the pure *Z* isomer is not directly accessible by kinetic measurements since the *Z* isomer can only be obtained as a mixture containing residual *E* isomer representing the photostationary state and thermal reversion to the thermodynamically more stable *E* isomer starts to contribute after prolonged reaction times. Therefore, initial kinetic data were corrected for reactivity attributed to residual *E* isomer and for thermal reversion of *Z* isomer to *E* isomer (Figure 5, Table 3).

In all cases, use of the reactive *Z* isomer of catalysts **1a**−**c** as well as **2** led to a rate enhancement as compared to the use of *E* isomer (Table 3). Catalyst **1a** displayed only a moderate difference in activity between its ON- and OFF-state, resulting in a relatively small value of $k_{rel} = 4.3$. It is evident from the kinetic data that use of the *E* isomer led to some residual activity not desirable for the OFF-state of a switchable catalyst. Most likely, the *E* isomer's reactivity originates from deprotonation of the nitroalkane, pointing to unwanted accessibility of the basic piperidine lone pair. Three pathways can be considered for the deprotonation of the nitroalkane by the catalyst's OFF-state: (1) inversion of the piperidine N-atom placing the lone pair in an equatorial position (i-**1a**−**c**), (2) chair flip leading to piperidine conformations with the basic lone pair in nonshielded equatorial or axial positions (f_{eq}-**1a**−**c** or f_{ax}-**1a**−**c**), and (3) a rotation of the blocking group allowing the nitroalkane to be deprotonated by the piperidine's most stable (chair) conformation with the lone pair in axial position. On the basis of computational and NMR studies (*vide supra*) the chair flip can be ruled out for catalysts **1a**−**c**. However, inversion of the nitrogen atom and/or rotation of the blocking group could in principle be responsible for residual catalytic activity of the OFF-state *E*-**1a** (Table 1).

In order to suppress *N*-inversion, the methyl group R was replaced with a more demanding *tert*-butyl group, known to act as an efficient conformational anchor for six-membered rings.[33] Indeed, N-inversion of the *E* isomer of catalyst **1b** could be ruled out by NMR spectroscopy as well as DFT calculations, which estimate a significant destabilization of i-**1b** over i-**1a** (Table 1). This leads to a roughly 200-fold decrease in population of the N-inverted isomer of catalyst **1b**, correlating with a significantly diminished residual activity, as compared to catalyst **1a**. In addition, the kinetic stability of i-**1b** is decreased due to the lowering of the N-inversion barrier as compared to that of i-**1a** (Table 1). Not unexpectedly, flipping of the piperidine chair is even more unlikely for **1b**. Investigation of the catalytic activity of catalyst **1b** in its ON- and OFF-state under identical conditions as used for **1a** revealed a significant improvement of the ON/OFF-ratio, reaching a value of $k_{rel} = 13.2$, corresponding to a reactivity difference of both switching states exceeding 1 order of magnitude (Table 3). The enhanced reactivity difference mainly originates from the pronounced decrease of the OFF-state's activity overcompensating the slightly reduced reactivity of the ON-state.[34]

Assuming the reactivity of *Z*-**1b** to be the maximum intrinsic reactivity of a *N*-*tert*-butyl-substituted piperidine, the catalyst's ON/OFF-ratio can only be improved by further lowering the reactivity of the OFF-state. This could be realized by improving the efficiency of blocking, provided by the azobenzene shield. Inspection of models of *E*-**1b** as well as **1b**-TSrot, obtained from DFT calculation, led to the initial conclusion that a twist of the blocking group around the C−N bond leads to a less shielded *E* isomer, potentially causing some residual reactivity. To address this problem, the R′ substituents of the blocking group responsible for shielding were increased in size, i.e. from *tert*-butyl (**1b**) to 2,6-dimethylphenyl (**1c**), taking advantage of our modular synthetic route (Scheme 1). Indeed, no rate acceleration was observed by using the catalyst's OFF-state *E*-**1c** as compared to the noncatalyzed reaction, while the reactivity of the ON-state *Z*-**1c** remained practically unaffected. Both effects led to an increased overall ON/OFF-ratio $k_{rel} = 35.5$.

It is interesting to note, that according to DFT calculations N-inversion of **1c** is energetically more favorable than inversion of **1b**, indicated by a decrease of the relative free enthalpy of the inverted isomers from 7.1 to 5.4 kcal/mol on going from **1b** to **1c** in the gas phase.[35] Obviously, the reactivities of the OFF-states cannot simply be explained by differences in populating the N-inverted conformers i-**1** and show that additional effects have to be taken into account. In order to address this rather complicated issue in more detail, we investigated the proton affinities (PAs) of the bases **1a**−**c** by computational methods. Representative calculated protonation energies and enthalpies are summarized in Table 4. Noting that the trends of the protonation energies in the gas phase are comparable for the two basis sets employed (compare ΔE/6-31G* and ΔE/cc-pVTZ values), we will discuss primarily the PAs obtained with the lower basis set. The latter are defined as the negative enthalpies of protonation of the free bases, i.e. the absolute value of the ΔH/6-31G* values of the protonated species in Table 4.

PAs of the global minimum conformation show a constant increase with increasing steric demand of the molecule on going from **1a** to **1c**. While the PA increases strongly on going from **1a** to **1b**, the difference between **1b** and **1c** is small, in line with the similar substitution at the piperidine nitrogen atom. Isomerization of the double bond leads to an increase of the

(32) Note that the higher concentration used in preparative irradiation experiments increased the absorbance of the solution such that usually even after prolonged irradiation times the photostationary-state mixtures contained a larger amount of *E* isomer as compared to irradiating analytical samples of much lower concentration. For these reasons, the conditions necessary to accurately determine the kinetics, i.e. the rather high catalyst concentrations employed in the NMR experiments, precluded switching of the catalysts in situ. However, this does only constitute a drawback in bulk or solution-phase catalysis associated with high optical densities—a drawback that photochemistry suffers from in general—yet an application utilizing mono-or multilayers of immobilized catalysts should be feasible.

(33) For a discussion of the conformational behavior of piperidines, see: Eliel, E. L.; Wilen, S. H. *Stereochemistry of Organic Compounds*; Wiley: New York, 1994, pp 740 and references therein.

(34) The reactivity of the *Z* isomer *Z*-**1b** was also lowered, most likely because the steric demand of the *tert*-butyl group hinders the nitroalkane to approach the basic catalyst site.

(35) At the B3LYP/cc-pVTZ/PCM(acetonitrile) level, the relative energies of i-**1a**, i-**1b**, and i-**1c** are 3.9, 7.1, and 5.8 kcal/mol, respectively, i.e. quite similar to the gas-phase ΔE values in Table 4.

Table 4. Relative Energies ΔE and Enthalpies ΔH Obtained at Selected Levels for Key Isomers of **1a**−**c** (with Respect to the Global Minimum, *E*-**1**), and Energies and Enthalpies of Protonation (Relative to the Respective Minima *E*-**1**, *Z*-**1**, i-**1**)[a]

	ΔE 6-31G*	ΔH (-PA)[b]6-31G*	ΔE cc-pVTZ	ΔE cc-pVTZ PCM(THF)[c]	ΔE cc-pVTZ PCM(MeCN)[d]
Z-**1a**	15.8	15.2	15.5	13.7	13.3
i-**1a**	3.8	3.8	4.4	4.0	3.9
E-**1a**H$^+$	−244.1	−234.5	−242.4	−276.0	−280.9
Z-**1a**H$^+$	−245.5	−235.6	−243.6	−281.8	−287.7
i-**1a**H$^+$	−245.1	−236.1	−243.8	−282.5	−288.4
Z-**1b**	15.4	15.2	15.0	13.6	13.2
i-**1b**	6.0	5.8	6.3	5.9	5.8
E-**1b**H$^+$	−250.5	−241.7	−248.5	−278.3	−282.8
Z-**1b**H$^+$	−251.7	−242.3	−249.5	−281.3	−286.5
i-**1b**H$^+$	−250.0	−240.3	−248.4	−282.5	−288.0
Z-**1c**	15.3	15.0	15.2	14.0	13.5
i-**1c**	5.5	5.4	6.0	5.9	5.8
E-**1c**H$^+$	−252.0	−242.4	−249.6	−278.9	−283.3
Z-**1c**H$^+$	−251.0	−241.5	−248.9	−281.2	−286.9
i-**1c**H$^+$	−250.6	−240.8	−249.1	−282.6	−287.7

[a] In kcal/mol, employing the B3LYP functional and B3LYP/6-31G* optimized geometries. [b] Negative PA for the protonated species (298.15 K, 1 atm). [c] Continuum model employing the parameters of THF. [d] Continuum model employing the parameters of acetonitrile.

PAs of **1a** and **1b** by 1.1 and 0.6 kcal/mol, respectively, whereas that of **1c** decreases by 0.9 kcal/mol upon $E \rightarrow Z$ isomerization. As the latter result cannot easily be rationalized on steric grounds alone, a potential explanation involves "internal solvation" of the protonated nitrogen center by the proximal R′ groups of the blocking moiety, which in the case of *E*-**1c**H$^+$ is somewhat more efficient due to a stabilizing interaction with the aromatic ring.[36] Upon solvation (modeled by a simple polarizable continuum), protonation of the *Z* isomers becomes much more favorable than that of the corresponding *E* isomers. Clearly, the protonated nitrogen center bearing the charge is more exposed to the solvent (or the continuum) in *Z*-**1**H$^+$, increasing their stabilization by favorable interactions with the solvent. This computed increase in basicity of *Z* vs *E* isomers is in qualitatve agreement with the experimental pK_a measurements discussed above, where both **1b** and **1c** show an increase in pK_a upon $E \rightarrow Z$ isomerization (Table 3). Quantitatively, this increase in basicity is significantly overestimated by the DFT/PCM calculations for acetonitrile as the computed differences in protonation energies are on the order of −4 kcal/mol (e.g., from −282.8 to −286.5 kcal/mol for **1b** in Table 4), which would translate into changes by several pK_a units. Evidently, the continuum solvation model is too simplistic and specific interactions with the solvent (or its dynamics) would have to be taken into account for a better quantitative accuracy.

When assessing the PAs of the N-inverted isomers, we assume that protonation equilibria are fast relative to N-inversion and discuss energetic differences between i-**1** and i-**1**H$^+$ (i.e., *N*-protonated i-**1**). Although N-inversion is so rapid that practically only equilibria involving the global minima *E*-**1** would be observable, the question of the inherent basicity of i-**1** is of interest in the context of catalysis, as the more reactive species (even when present in small amounts) might constitute the more potent catalysts. In the gas phase, i-**1a** is indicated to be a stronger base than *E*-**1a**, whereas the opposite is found for i-**1b**,**c**. Steric reasons are likely to be responsible for this result, because the repulsion between the R and R′ groups is so strong in i-**1b**,**c** that the amine nitrogen atom is significantly planarized, i.e. the angle sum at N amounts to 352° in both cases. When going from i-**1a** (angle sum of 339°) to i-**1b**,**c**, the s-character of the nitrogen lone pair and hence its basicity are decreased. In the polar continuum, this effect is overcompensated by the better stabilization of the i-**1**H$^+$ isomers with their solvent-accessible cationic NH centers, and all i-**1** forms are computed to be stronger bases than their *E*-**1** counterparts.[37]

To summarize this part, the higher basicity of the inverted isomer of **1a** might account to some extent for the significant reactivity of the OFF-state, since a thermal population of the N-inverted isomer is possible. Even if the population of i-**1a** is small (at 298 K, a relative free energy of 4 kcal/mol would correspond to 0.1% in an equilibrium mixture), its contribution to the overall catalytic turnover would be noticeable because of the expected enhanced reactivity. Freezing the N-inversion by incorporation of the *tert*-butyl group lowers the population of the *N*-inverted isomers of **1b** and **1c** even more, thus strongly reducing their potential contribution to the residual activity. This interpretation is consistent with the experimental results, provided the relative reactivities reflect the respective thermodynamic driving forces (for a discussion of possible kinetic effects see below). By comparing catalysts **1b** and **1c**, it is evident that no further improvement of the activity ratio k_{rel} seems possible for the particular system under investigation. As mentioned, the reactivity of *Z*-**1b** and *Z*-**1c** represents the intrinsic reactivity of a *N*-*tert*-butyl-substituted piperidine incorporated into the catalysts framework toward nitroethane, leaving no room for further improvement since a greater extent of deshielding is not possible. The lower limit of reactivity is given by *E*-**1c** displaying a reactivity not distinguishable from the reaction's background reactivity.

Since slow thermal reversion of the *Z* isomers of catalysts **1a**−**c** leads to unwanted catalyst deactivation upon prolonged reaction times, stilbene-based catalyst **2** was devised to suppress thermal $Z \rightarrow E$ isomerization. Comparison of DFT-optimized structures of azobenzene-based catalysts *E*-**1a** and *E*-**2** reveals interesting differences.[7] On going from the azobenzene to the stilbene, the elongation of the X═X distance and the opening of the X═X−C angle (115° and 126° for X = N and C, respectively) strongly increases the separation between the amine N-atom and the *tert*-butyl substituent of the blocking group, and is expected to lead to less efficient shielding and a higher reactivity of the *E* isomer. This was confirmed experimentally, observing a 2.6 times higher reactivity for *E*-**2** as compared to *E*-**1a** under otherwise identical conditions. Switching stilbene **2** to its corresponding *Z* isomer only moderately accelerated the rate of the reaction, i.e. $k_{rel} = 2$. In addition to this low ON/OFF-ratio the applicability of stilbene **2** as a photoswitchable catalyst is further narrowed by the inefficient photochemical $Z \rightarrow E$ isomerization (*vide supra*).

In their OFF-state, catalysts **1b** and **1c** display a distinct difference in reactivity in the Henry reaction, even though they

(36) (a) Hunter, C. A.; Lawson, K. R.; Perkins, J.; Urch, C. J. *J. Chem. Soc., Perkin Trans. 2* **2001**, 651–669. (b) Meyer, E. A.; Castellano, R. K.; Diederich, F. *Angew. Chem., Int. Ed.* **2003**, *42*, 1210–1250.

(37) For i-**1a**, this stabilization is predicted to be so strong that the protonated inverted isomer i-**1a**H$^+$ is even more stable than *E*-**1a**H$^+$. This particular result should be taken with care in light of the performance of the continuum model for predicting the basicities of *Z* vs *E* isomers (*vide supra*). However, the qualitative finding that the N-inverted isomers i-**1** are more basic than their more stable chair conformers *E*-**1** forms should be reliable.

have almost equal basicities in acetonitrile. This observation suggests that under catalytic turnover, dictated by the kinetics of the rate-limiting step, the reaction barriers are influenced by other factors in addition to those solely grounded on thermodynamic driving forces for substrate deprotonation. The rate-determining step in the general-base catalyzed Henry reaction is the deprotonation of the nitroalkane by the amine base. The conformational flexibility of the systems under scrutiny as well as the need to properly account for solvation effects during the concomitant charge separation make a computational search for the relevant transition states for deprotonation very involved.[38] As a first step, representative adducts formed from *E*-**1a**−**c** and the simplest nitroalkane, nitromethane, which are likely to be involved in the early stages of deprotonation, were located (Figure 6). The raw nitromethane-complexation energies, uncorrected for zero-point energies and basis-set superposition error, are −4.0, −3.1, and −2.4 kcal/mol for **1a**, **1b**, and **1c**, respectively. As can be seen in the optimized structures in Figure 6, the blocking group has to rotate significantly about the C−N bond in order to allow coordination of the nitromethane to the lone pair. For a more quantitative analysis, the energies required to distort the free bases from their conformations in the fully optimized global minima to those in the nitromethane complexes were evaluated. These energies should be a good indication of the kinetic hindrance imposed by the substituents R and R′ during the deprotonation step and amount to 1.4, 2.3, and 3.6 kcal/mol for **1a**, **1b**, and **1c**, respectively. These data are in very good qualitative agreement with the experimentally observed reactivity trend for the OFF-states of **1a**−**c**. The rather low energetic "penalty" for coordination of the nitroalkane to *E*-**1a** is noteworthy, as it implies that a substantial part of the residual activity of **1a** in its OFF-state is in fact due to the global *E* minimum itself, in addition to the part that may arise from traces of the N-inverted isomer (*vide supra*). Even though it is beyond the theoretical methods presently available to relate these rather modest changes in the energetics quantitatively to specific rate constants, the overall qualitative agreement between theory and experiment provides a solid basis for our interpretation of the observations.

In the general context of comparing the competing reactivities of an equilibrating mixture of conformers, we most likely deal with a scenario in which the activation barriers for interconverting the participating conformers, i.e. *E*-**1**, i-**1**, f_{ax}-**1**, and f_{eq}-**1**, are comparable to the activation barriers for proton abstraction from a nitroalkane.[38] For this reason, the simplest case of the reactivity schemes, developed by Winstein and Holness on the basis of kinetic observations as well as Curtin and Hammett on the basis of product distributions,[39] probably does not apply and our system would be more appropriately described by the general treatment given by Seeman and Farone.[40]

Conclusion and Outlook

In conclusion, we have developed a new conceptual design for photoswitchable catalyst systems. Photoswitchable catalysts on the basis of conformationally locked piperidine bases were synthesized and differences in basicity of the switching states involved were successfully exploited to photocontrol the catalysts' activities in general base catalysis, exemplified by photocontrolling conversion of the Henry reaction. A careful analysis of the dynamic structural behavior in solution using the recently introduced residual dipolar couplings enabled us to establish the structure−reactivity relation for the catalyst system, thereby facilitating tuning of the catalysts to enhance ON/OFF-ratios. Current work in our laboratory is directed toward surface tethering of the catalyst, potentially offering unprecedented applications in surface patterning and functionalization. Extension of our concept to intrinsically more reactive catalysts with better ON/OFF-ratios, potentially allowing for photocontrol of chemical selectivities and polymerization processes, constitutes a challenging target for future research. With such "smart" catalysts in hand, new responsive and adaptive materials can be envisioned.

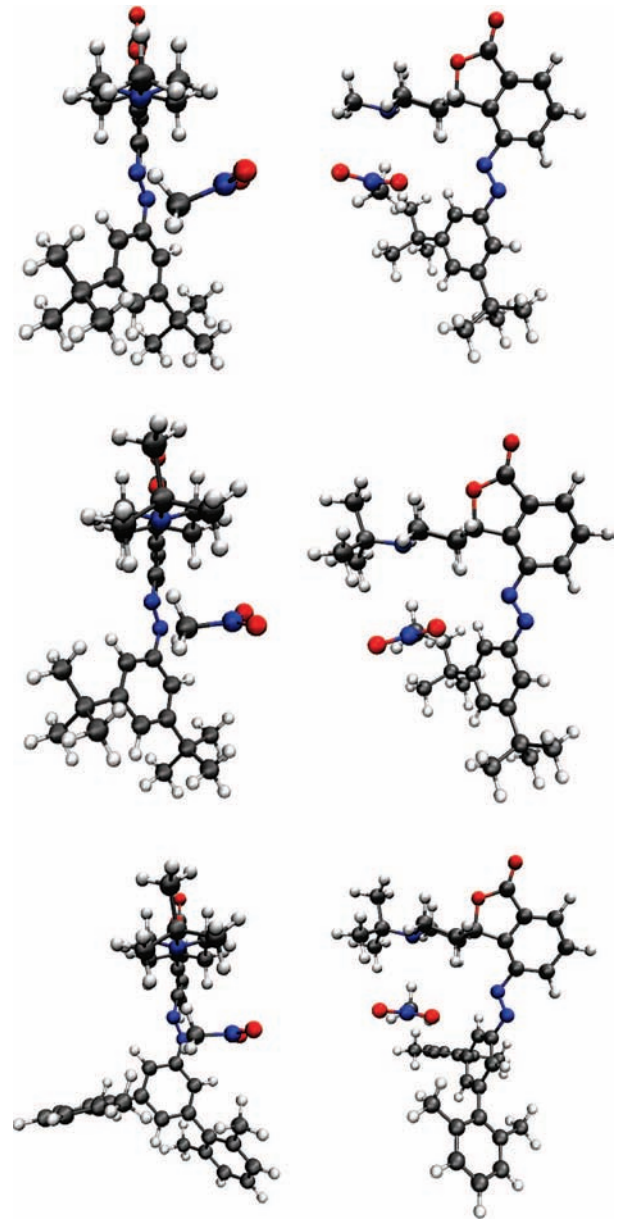

Figure 6. Adducts between nitromethane and E-**1a**−**c** illustrating the degree of twisting of the aromatic blocker group (left: front view along the N-R axis, right: side view; B3LYP/6-31G*optimized).

(38) In a recent B3LYP study of the Henry reaction catalyzed by a cinchona alkaloid, a barrier of 10.8 kcal/mol for deprotonation of nitromethane has been computed in a THF continuum: Hammar, P.; Marcelli, T.; Hiemstra, H.; Himo, F. *Adv. Synth. Catal.* **2007**, *349*, 2537–2548.

(39) For comprehensive reviews on the effect of conformational changes on reactivity in organic chemistry, see: (a) Seeman, J. I. *Chem. Rev.* **1983**, *83*, 83–134. (b) Reference 33, pp 647−655.

(40) Seeman, J. I.; Farone, W. A. *J. Org. Chem.* **1978**, *43*, 1854–1864.

Acknowledgment. We thank Petra Neubauer and Dr. Burkhard Ziemer (HU Berlin) for carrying out the single crystal X-ray structure analyses. Generous support by the German Research Foundation (DFG via SPP 1179 and Emmy Noether Program TH1115/3-1) and the Fonds der Chemischen Industrie is gratefully acknowledged. M.B. thanks EaStChem for support. RSS is indebted to the Studienstiftung der deutschen Volkes for providing a doctoral fellowship. Wacker Chemie AG, BASF AG, Bayer Industry Services, and Sasol Germany are thanked for generous donations of chemicals.

Supporting Information Available: Synthetic and computational details, compound characterization data, NMR experiments and data analysis including measured RDCs and fitting details as well as optimized Cartesian coordinates of all structures and selected three-dimensional plots thereof. This material is available free of charge via the Internet at http://pubs.acs.org.

JA807694S